ORIGINAL PAPER

Local calcium signals induced by hyper-osmotic stress in mammalian skeletal muscle cells

**Simona Apostol · Daniel Ursu ·
Frank Lehmann-Horn · Werner Melzer**

Abstract Strenuous activitiy of skeletal muscle leads to temporary osmotic dysbalance and isolated skeletal muscle fibers exposed to osmotic stress respond with characteristic micro-domain calcium signals. It has been suggested that osmotic stress targets transverse tubular (TT) dihydropyridine receptors (DHPRs) which normally serve as voltage-dependent activators of Ca release via ryanodine receptor (RyR1s) of the sarcoplasmic reticulum (SR). Here, we pursued this hypothesis by imaging the response to hyperosmotic solutions in both mouse skeletal muscle fibers and myotubes. Ca fluctuations in the cell periphery of fibers exposed to osmotic stress were accompanied by a substantial dilation of the peripheral TT. The Ca signals were completely inhibited by a conditioning depolarization that inactivates the DHPR. Dysgenic myotubes, lacking the DHP-receptor-alpha1-subunit, showed strongly reduced, yet not completely inhibited activity when stimulated with solutions of elevated tonicity. The results point to a modulatory, even though not essential, role of the DHP receptor for osmotic stress-induced Ca signals in skeletal muscle.

Keywords Mouse muscle fibers · Myotubes ·
Transverse tubular system · Dihydropyridine receptor ·
Confocal calcium imaging · Osmotic stress

S. Apostol · D. Ursu · F. Lehmann-Horn · W. Melzer (✉)
Institute of Applied Physiology, Ulm University,
Albert-Einstein-Allee 11, 89069 Ulm, Germany
e-mail: werner.melzer@uni-ulm.de

S. Apostol
Physics Department, Faculty of Sciences and Arts,
Valahia University, 24 Bd. Unirii, 0200 Targoviste, Romania

Introduction

Skeletal muscle cells respond to action potential (AP) depolarization with a rapid, almost uniform increase of their cytoplasmic calcium concentration. The release of Ca stored in the sarcoplasmic reticulum (SR) is controlled by voltage-sensitive L-type Ca channels (dihydropyridine receptors, DHPRs) located in the membrane of the transverse tubules (TTs) that conduct the AP from the surface to the center of the cell. The DHPRs trigger the opening of ryanodine receptors (RyR1) in the SR membrane by means of a direct mechanical link (for reviews see Melzer et al. 1995; Dulhunty 2006). Experiments on frog skeletal muscle revealed a quantal substructure of the voltage-controlled Ca transients as an unexpected and important feature of the excitation–contraction (EC) coupling mechanism (Klein et al. 1996). The quanta, termed "sparks" can be studied in isolation at rest or at low activation levels (Shirokova et al. 1999a; Klein and Schneider 2006). In contrast to amphibian skeletal muscle fibers, intact mammalian fibers normally show no spontaneous Ca sparks and depolarization recruits elementary events of smaller amplitude, named "embers" that probably result from the opening of individual ryanodine receptors (Zhou et al. 2003; Csernoch et al. 2004). They do, however, produce sparks when the intracellular space is exposed to artificial solutions after mechanical ablation of the plasma membrane or permeabilizing plasma membrane and TTs (Kirsch et al. 2001). Studies on immature myocytes in culture showed that sparks occurred preferentially in TT-free regions where the voltage-controlled Ca release was not functional, indicating a role of the TT system and the DHPR voltage sensors in silencing spontaneous Ca sparks (Shirokova et al. 1999b; Zhou et al. 2006).

In frog muscle, Ca phenomena ranging from spark-like spatially restricted events to oscillations and waves could be demonstrated in response to solutions with increased osmolarity (Chawla et al. 2001; Martin et al. 2003). Later Wang et al. (2005) showed that enzymatically dissociated mouse muscle fibers likewise exhibit local Ca signals under these conditions and that fibers isolated from the mdx mouse, an animal model for muscular dystrophy, show dramatically enhanced activity. Both application of hyper-osmotic solution and the return to iso-osmotic solution after a brief hypo-osmotic challenge induced similar local signals (Wang et al. 2005). The authors proposed a mechanism in which osmotic stress weakens a constitutive inhibitory control of the DHPR on the ryanodine receptor (RyR1) thus leading to spark activity. In a subsequent study, Martins et al. (2008) presented evidence for an involvement of reactive oxygen species generated by NADPH oxidase in the formation of the tonicity-induced Ca signals. Based on experiments investigating the tonicity-induced response in muscle fibers of the dystrophic mdx mouse Teichmann et al. (2008) suggested mechano-sensitive ion channels interacting with the DHP receptors within a common macromolecular signaling complex that is stabilized by cytoskeletal elements including dystrophin.

The specific aims of the present study were (1) to characterize the tonicity-induced Ca signals by comparing their spatio-temporal parameters under different triggering conditions, (2) to investigate structural changes that accompany the local Ca signals, (3) To compare mature muscle fibers with developing myocytes regarding the response to osmotic stress, and (4) to test the hypothesis of DHPR involvement by studying chronically depolarized muscle fibers and DHPR-deficient myocytes.

Materials and Methods

Muscle cell preparations

Balb/c and Sv129/J mice (age 2–6 months) were sacrificed by exposure to CO_2, followed by cervical dislocation, in agreement with the guidelines of the local Animal Care Committee. The interosseus muscles were excised from the hindlimbs, and subjected to enzymatic dissociation at 37°C for 60 min using a Krebs–Ringer solution containing 2 mg/ml type I collagenase (Sigma-Aldrich). Fibers loosely attached to the cover slip bottom of the recording chamber were loaded using 5 μM Fluo-4-AM (60 min, room temperature). Experiments commenced after washing out the dye from the chamber with isotonic Ringer's solution followed by 15 min of equilibration. In some experiments, the impermeable and hydrophobic dye FM 4–64 was added to the bathing solution (5 μg/ml) to label

the plasma membrane and TT system (Vida and Emr 1995). Both dyes were purchased from Invitrogen-Molecular Probes. In addition, muscle fibers cut at both ends were manually dissected from the extensor digitorum longus (EDL) in relaxing solution using fine scissors and tweezers and fixed in the recording chamber by metallic clips covered with silicone. Fibers were stretched to a sarcomere length of 3–3.7 μm and were permeabilized by a 2 min exposure to *internal solution* containing 0.01% saponin followed by washing with *internal solution* containing the potassium salt of the fluorescent dye Fluo-4 (100 μM). For experiments on myotubes we used two murine cell lines: (1) C2C12 which show normal voltage-activated L-type Ca inward current and Ca release (Schuhmeier et al. 2003; Schuhmeier and Melzer 2004) and (2) GLT (Powell et al. 1996), derived from homozygous dysgenic (mdg) mice, which lack the dihydropyridine receptor α_{1S} subunit and show no Ca response to depolarization. Myotubes were cultured as described (Schuhmeier et al. 2003, 2005). Cells were plated on carbon- and gelatin-coated coverslips loaded with 5 μM Fluo-4-AM in isotonic Ringer solution (20 min; 37°C). The coverslips with the adherent cells were then attached to the bottom of a Plexiglas chamber and equilibrated for at least 15 min in isotonic Ringer's solution.

Solutions

Cells were bathed in isotonic *Ringer's solution* containing (mM) 140 NaCl, 2 $MgCl_2$, 2.5 $CaCl_2$, 10 HEPES, 5 KCl, pH 7.4, ~290 mOsm. During experiments the bath solution was refreshed every 30 min using a home-made perfusion system. For local stimulation, solutions were pressure-ejected from a micropipette positioned close to the cell surface under the control of computer-gated magnetic valves. Pipettes were pulled from borosilicate glass (GB150TF10, Science Products, Hofheim, Germany) using a commercial patch pipette puller (DMZ, Zeitz Instruments, München, Germany). Hypertonic solutions were prepared by increasing the osmolarity to ~420 mOsm using either 50 mM $CaCl_2$ (*Ca-HyO*), as described by Wang et al. (2005) or by adding 120 mM sucrose (*S-HyO*). In other experiments mannitol or glucose were used instead of sucrose. The osmolality was checked with a cryoscopic osmometer (Osmomat 030, Gonotec, Berlin, Germany). In experiments to depolarize the membrane to close to 0 mV, an isotonic solution (*High-K*) with the following constituents was used (mM): 16 KCl, 92 K_2SO_4, 7.6 $CaSO_4$, 1 $MgSO_4$, 11 Glucose, 40 Sucrose, 2 TES, pH 7.4, ~290 mOsm. Solutions used for experiments with permeabilized fibers had the following constitution: *Relaxing solution* (mM): 140 K glutamate, 10 $MgCl_2$, 0.3 $CaCl_2$, 10 HEPES, 1 EGTA, 5 glucose, pH 7.0 balanced with KOH.

Internal solution (mM): 140 K glutamate, 4.5 $MgCl_2$ (0.6 mM free Mg^{2+}), 0.096 $CaCl_2$ (100 nM free Ca^{2+}), 10 HEPES, 0.5 EGTA, 5 glucose, 5 Na_2ATP, 5 Na_2 creatine phosphate, 0.1 K_5-fluo-4, pH 7.0 balanced with KOH.

Confocal microscopy

Experiments were performed using a Radiance 2000 confocal scanner (Bio-Rad Cell Science Division, Hemel Hempstead, UK) adapted to an Eclipse T300 inverted microscope (Nikon, Tokyo, Japan). For Ca imaging with Fluo-4 we used a $60\times$ oil immersion objective (PlanApo, $60\times$, 1.4 N.A.; Nikon). The spatial resolution was estimated as 0.25 μm in the x and y dimensions, and 0.5 μm in the z dimension. Fluorescence was excited by the 488 nm laser line and collected using a bandpass HQ520/30 or a longpass HQ500LP emission filter. For membrane staining with FM 4-64 we used a HQ600LP emission filter. In the xy-scanning mode a series of 100–200 images (512×512 pixels, 750 lines s^{-1}) was acquired at about 1.46 Hz repetition frequency. Generally, transmission images were recorded simultaneously with the confocal fluorescence images. Line scans (xt-images) contained 512 pixels in space ($\sim$94.9 μm) and 1,024 pixels in time (repetition intervals 1.333, 2.000 or 6.024 ms). Within a pre-defined region of the fiber, the position of the line was randomly changed after each image acquisition to avoid photodynamic damage. All experiments were conducted at room temperature ($21 \pm 1°C$).

Image analysis

Lines showing the lowest fluctuations in intensity were automatically selected and their average used for background subtraction. The difference image was normalized by the background ($\Delta F/F_0$). After filtering and setting a threshold criterion of 0.6 times the standard deviation of the normalized raw image, a binary image was generated highlighting the detected signals (super-threshold events covering at least 50 pixels). The parameters amplitude ($\Delta F/F_0$), full width at half-maximum (FWHM) and full duration at half-maximum (FDHM) were evaluated for the detected events using the normalized difference image. For myotubes a semi-automatic detection, guided by visual inspection, was applied. In some figures we present space-time images that were constructed from a series of xy-scans using a specified rectangular region of interest (ROI). The pixel intensities in one dimension of the ROI were averaged thus condensing the rectangle to a line exhibiting the averaged intensity profile. The lines were then assembled in chronological order producing the final space-time image (crop image). To determine global fluorescence increase, we averaged the pixel intensities in large ROIs covering cytoplasmic regions (excluding nuclei). The average from 10 frames recorded before the stimulus was used for normalization. To determine the cytoplasmic area free of nuclei in xy images of myotubes we used a combination of Matlab (The MathWorks, Natick, Massachusetts, USA) and Adobe Photoshop (Adobe Systems, München, Germany) tools.

Statistics

Unless otherwise stated, averaged data are presented and plotted as means $\pm$ SEM (n = number of experiments). Student's two-sided t test was used to test for significant differences of mean values. $\Delta F/F_0$ and FDHM were also tested using the non-parametric Mann–Whitney U-test.

Results

Triggering local Ca signals by osmotic stress

To investigate osmotic stress-induced calcium signals, we used local perfusion from a micropipette positioned close to the muscle fiber as demonstrated in Fig. 1A. The pressure-ejected hyperosmotic solution caused a decrease in fiber diameter which could be determined from a series of transmission images as shown in Fig. 1A and B. Simultaneously fluo-4 fluorescence images were recorded to determine myoplasmic changes of the Ca concentration (Fig. 1C–E). As described by Wang et al. (2005), spark-like events appeared in the periphery of the fiber in a region of 10–15 μm from the surface (Fig. 1D). Kirsch et al. (2001) termed the local Ca events identified by them in skinned mammalian skeletal muscle fibers "elementary calcium release events" (ECRE) to distinguish them from the brief and stereotyped sparks of amphibian muscle. We adopt this terminology for the heterogeneous signals described here acknowledging that their mechanism of formation may be different. Figure 1E is a space-time image constructed from crops of a series of xy-frames and shows the temporal evolution of fluorescence intensity (z-axis) at the border of the fiber segment. Figure 1F exemplifies the quantification of the changes observed during exposure to a hyperosmotic solution according to Wang et al. (2005). The fiber diameter change in the transmission images (Fig. 1B) was recorded using an automatic edge detector and was converted to the fractional change in volume (trace a) by normalizing to the averaged values obtained from 10 images before stimulation. The fluorescence images were analyzed in two ways: (1) by determining the global increase in fluorescence within a rectangular ROI covering almost the entire visible fiber image (trace b) and (2) by counting the ECRE per frame (diagram c).
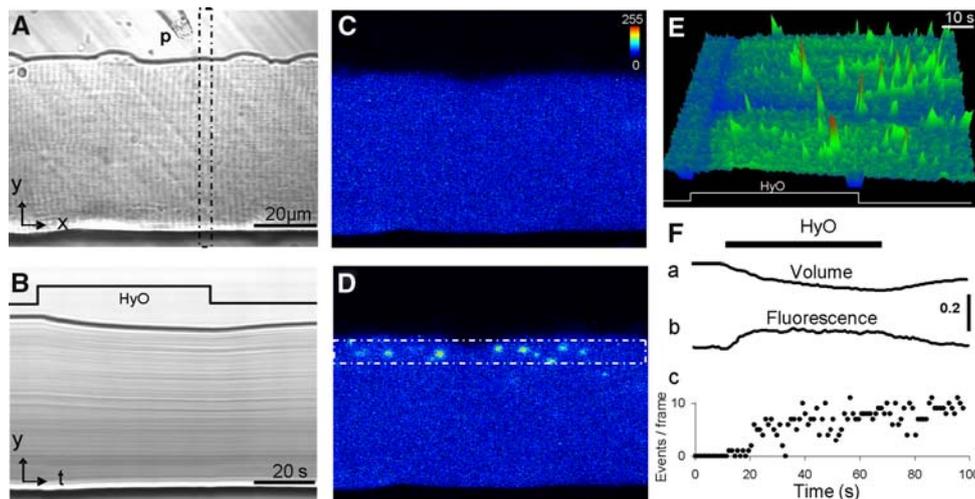
Fig. 1 Local calcium changes induced by hyperosmotic stimulation in muscle fibers. **A** Transmission image of a mouse interosseus muscle fiber (*x* and *y* indicate longitudinal and transversal axes of the fiber). *P* indicates the tip of the pipette used for application of hyperosmotic solution (Ca-HyO). **B** Space–time (*xt*) image generated from crops (dashed frame in **A**) of 100 *xy* images demonstrating the time course of the fiber diameter change during stimulation. **C**, **D** Confocal Fluo-4 fluorescence images (*xy*-mode) of the same fiber before (**C**) and after hyperosmotic stimulation (**D**) demonstrating the triggering of ECRE. *Note*: The focal plane was positioned in the center of the fiber. **E** 3-Dimensional presentation of fluorescence intensity changes in the periphery of the fiber segment (length 94.5 μm). The time course was constructed by stringing together intensity profiles obtained from narrow ROIs (marked by the *dashed lines* in **D**) as described in Methods. **F** Time plots of changes in fiber volume *a*, global fluorescence *b* and ECRE activity *c*. Volume and cytoplasmic fluorescence were normalized to their initial values before the solution change

Figure 2A shows pooled results from several experiments similar to the one in Fig. 1 which responded with ECRE activity. As the global increase can mask the local Ca release, we chose only experiments for this figure in which local Ca release events could still be well distinguished despite the rising background fluorescence. On average, the fractional volume decrease induced by the hyperosmotic solution reached 15 ± 2%. A similar value (17 ± 2%) and similar kinetics (half times of 10–15 s) were obtained for the increase in global fluorescence, indicating that it mainly results from the concentrating effect caused by the volume reduction. The maximum value of the ECRE activity of about five events per frame (panel c) corresponds to a mean ECRE density in each frame of about $0.005/\mu m^2$ in the 10 μm wide active peripheral region.

In the experiments of Fig. 2A we used a solution as described in the original report by Wang et al. (2005), i.e. osmolarity was increased by adding 50 mM $CaCl_2$ to the normal Ringer solution. Because these conditions increase the inward driving force for Ca and external ionic strength, we also used uncharged substances to raise osmolarity to equivalent values (120 mM sucrose, glucose or mannitol). The analysis is shown for sucrose (S-HyO) in comparison to $CaCl_2$ (Ca-HyO) in Fig. 2. As a consistent and surprising difference, the global increase in fluorescence that occurred in addition to the ECRE activity (row b) was considerably
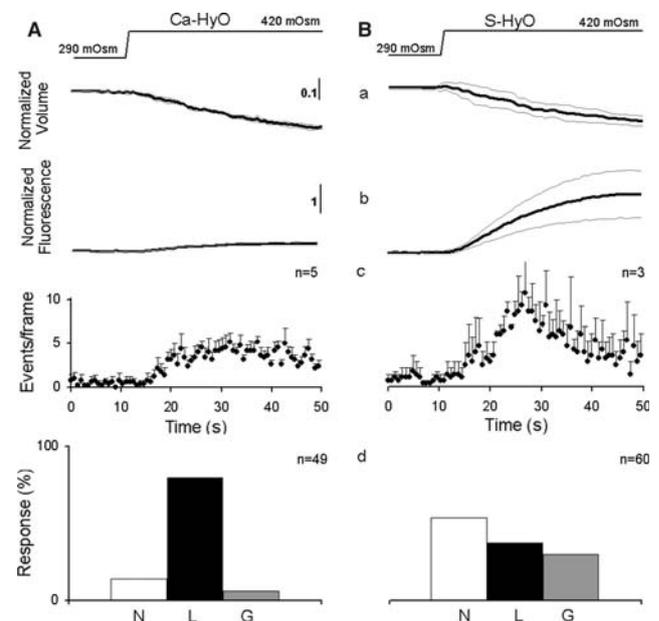

Fig. 2 Summary of Ca signal activity during hyperosmotic stimulation. Pooled results of muscle fiber responses to local superfusion as described in Fig. 1 using Ringer's solutions made hyperosmotic by adding 50 mM $CaCl_2$ (Ca-HyO) (**A**) as in Wang et al. (2005) or by adding 120 mM sucrose (S-HyO) (**B**). The *upper traces* indicate the instance at which pressure was applied to the micropipette to eject the solution. Averaged recordings of fractional volume change *a*, fractional increase in global fluorescence *b* and ECRE activity *c* as described in Fig. 1F. Thin lines and error bars indicate SEM. Cell responsiveness *d*; see text for explanation

larger when the uncharged osmolytes were used. The mean fractional increase in global fluorescence in the case of sucrose (S-HyO) was $110 \pm 40\%$ compared to a mean decrease in volume by $12 \pm 2\%$.

Further differences can be noticed from the panels in row d of this figure in which the responsiveness of the cells is detailed. The columns labeled N, L and G represent the percentage of cells responding not at all (N), with local Ca ECRE (L) and with a clearly noticeable global increase in fluorescence (G), respectively. Here, a global increase in fluorescence of more than 50% of the initial value was considered a positive response. Cells showing no ECRE and a global fluorescence increase of less than 20% were regarded as non-responsive. The result shown in the panels of row d confirms that a higher number of cells responded with a strong global increase in fluorescence to S-HyO application. On the other hand, a lower percentage of cells showed ECRE responses and the fraction of non-responders was considerably larger.

In a separate series of experiments we applied solutions of different osmolarities ranging from 330 to 440 mOsm (adjusted with sucrose). The results are summarized in Fig. 3. They show that osmolarities above 400 mM are required to induce a robust response, but a certain, relatively small percentage of the cells showed ECRE already at the lowest osmolarity increase.

Figure 4 shows representative line scan recordings and frequency histograms for the parameters $\Delta F/F_0$, FWHM and FDHM. Figure 4A shows results from permeabilized
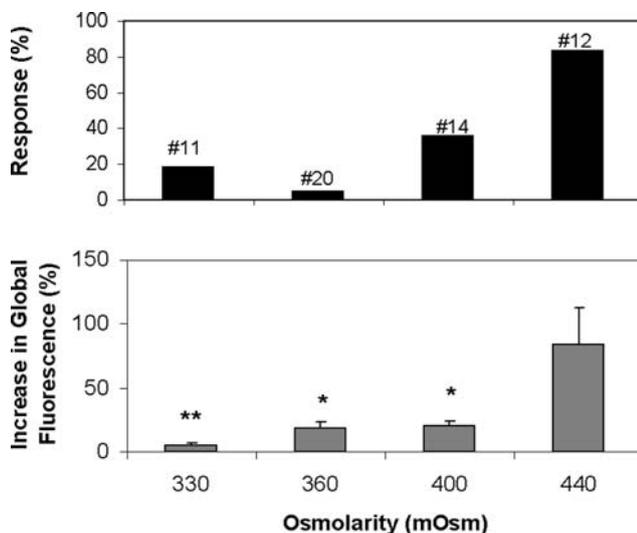
fibers treated as described in Kirsch et al. (2001), whereas Fig. 4B and C present data from isolated intact interosseus fibers stimulated with Ca-HyO and S-HyO, respectively. To better resolve also extremely long lasting events which were rarely observed in the permeabilized fibers but were characteristic of fibers exposed to osmotic stress, we increased the recording time by lowering the scanning frequency from 750 lines/s to 500 and 166 lines/s (number of lines per frame kept constant at 1,024; note the different time scales in the xt-images). The histograms corresponding to the fast, medium and slow scanning modes are displayed in white, gray and black, respectively. The parameter values determined in these experiments are summarized in Table 1.

Morphological changes of the TT system during osmotic stress

A likely reason for the restriction of ECRE to the periphery of the muscle fibers is that the tonicity-induced deformation remains confined to this region. Therefore, we searched for local structural changes occurring in parallel with the local calcium signals. Transmission images of osmotically challenged muscle fibers showed a conspicuous "graininess". In confocal images of fluo-4-loaded fibers this structural change could be attributed to the appearance of vacuoles within the fiber devoid of dye fluorescence. Staining the plasma membrane and its transverse tubular invaginations with the dye FM4-64 (Fig. 5A, red color) revealed that the vacuoles resulted from alterations in the TT system. Figure 5B shows a sequence of image crops from xy-scans recorded at different times within a one minute interval after application of the hyperosmotic solution. The arrows point to the fluorescently labeled tubules. It can be noticed that the regular double row pattern of the TT system gets deranged by growing dark areas. Applying a non-permeant fluorescent dye (fluo-4 salt) to the extracellular space (green color, Fig. 5C) showed that the empty spaces became filled with the dye demonstrating their continuity with the extracellular space and identifying them as dilated T-tubules. Like the ECRE, the TT swelling events were most evident in the peripheral regions of the fibers. Furthermore, the simultaneous recordings of changes in membrane morphology and intracellular Ca are compatible with a causal relationship between the two events. Figure 5D shows two xy-scans of a series of recordings from a FM4-64-stainded fiber loaded with fluo-4-AM (merged images) that contains examples of tonicity-induced ECRE at locations which half a minute later (panel b) showed strong TT dilation. The time course of the changes in the region indicated with the arrow in panel a is depicted in Fig. 5E. It was constructed by using narrow crops from a sequence of 80 consecutive recordings. Panel
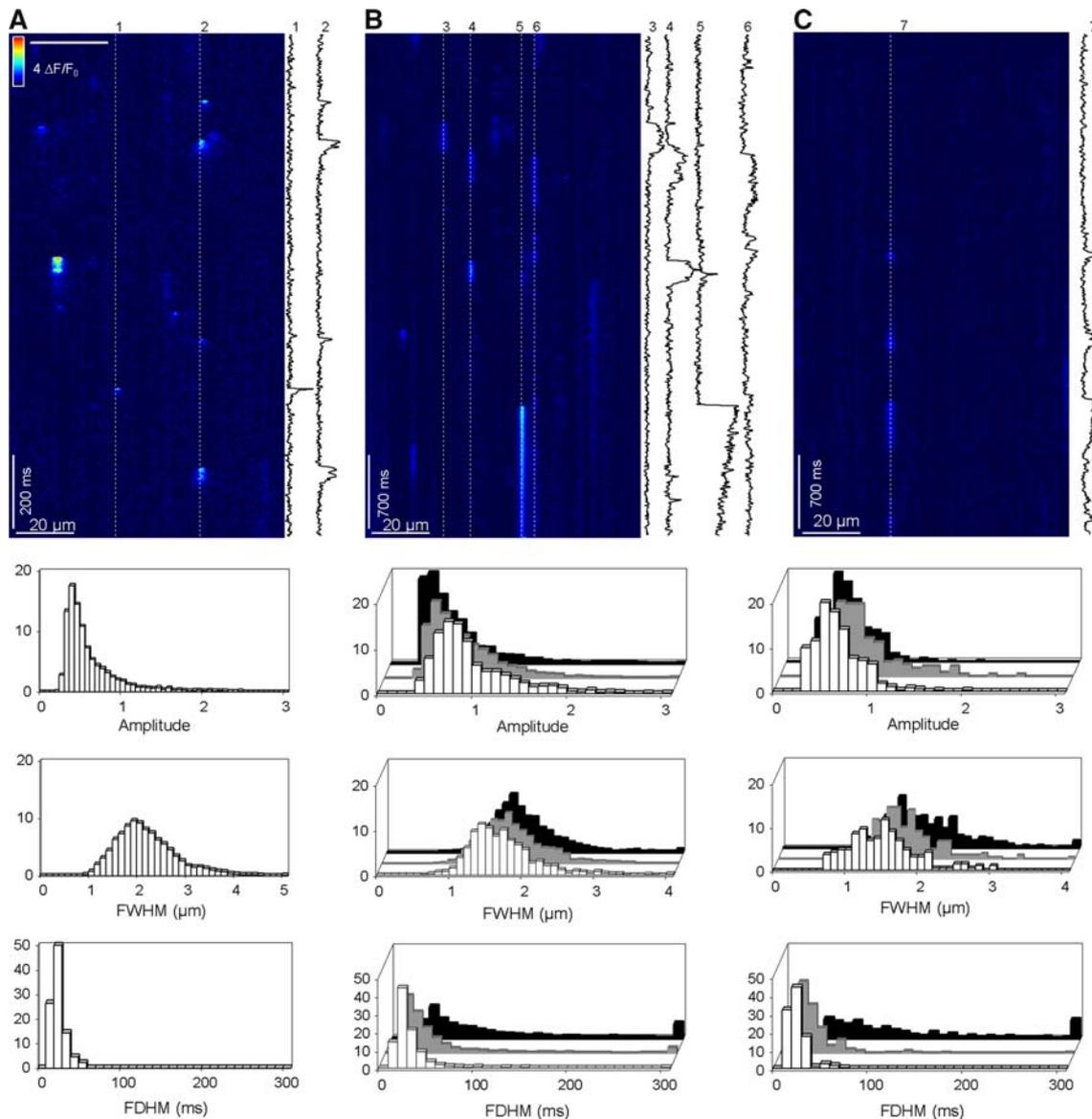
Fig. 3 Response of muscle fibers to different extracellular tonicities Percentage of fluo-4-loaded cells showing ECRE (*upper panel*) and fractional increase in global fluorescence (*lower panel*) in response to Ringer's solutions with different osmolarity (ranging from 330 to 440 mOsm). Numbers of cells tested are indicated. Asterisks indicate a significant difference to the highest concentration (* $P < 0.05$, ** $P < 0.01$)

Fig. 4 Comparison of ECRE morphology in permeabilized fibers under isosmotic conditions and in intact fibers subjected to hyperosmotic solutions Line scan images and frequency histograms of ECRE parameters (see text). *Note*: Events reaching beyond the image boundaries were not counted. Records are from a saponin-permeabilized EDL fiber (**A**) and from intact interosseus muscle fibers stimulated with Ca-HyO (**B**) and S-HyO (**C**). The traces on the right of each panel show the time course of the fluorescence changes at the positions indicated by the dashed lines (numbers 1–7)

a is the fluo-4 image showing the Ca increase at the onset of the emerging empty space and panel b the FM4-64 image demonstrating that the empty space originates from one of the double bands representing transverse tubules.

Global and local Ca response to osmotic stress are suppressed by fiber depolarization

To explain the osmotic stress-induced Ca signals, Wang et al. (2005) suggested that mechanical perturbation caused relief from a constitutive inhibition of the RyR1 Ca release channels by their DHPR voltage sensor leading to local release of Ca from the SR. A goal of our study was to obtain experimental evidence for or against this hypothesis.

A long lasting depolarization converts the DHPR to an inactivated state and prevents voltage-sensitive Ca release. We tested whether a depolarization that produces DHPR inactivation suppressed tonicity-induced local Ca signals. For this purpose, we applied a modified Ringer's solution (*High-K*) in which the major cation was potassium and the major anion sulfate (Methods, Dulhunty 1991). After 20 min in the depolarizing solution, fibers were focally

Table 1 Morphology of ECRE in muscle fibers

Condition	Event parameters (xt-images)					Event density (xy-images)	
	Speed (lps)	Amplitude ($\Delta F/F_0$)	FWHM (µm)	FDHM (ms)	N	Events/frame	N
Ca-HyO	750	0.88 ± 0.01	1.64 ± 0.02	26.10 ± 1.23	951	4.87 ± 0.04	5,485
	500	0.75 ± 0.01	1.72 ± 0.01	45.61 ± 0.83	2,091		
	166	0.58 ± 0.01	1.84 ± 0.01	119.83 ± 3.58	1,955		
S-HyO	750	1.03 ± 0.03	1.43 ± 0.04	15.52 ± 0.75	189	4.16 ± 0.05	2,943
	500	0.81 ± 0.02	1.66 ± 0.03	31.97 ± 2.53	221		
	166	0.58 ± 0.01	1.94 ± 0.04	144.91 ± 9.52	388		
Permeabilized	750	0.56 ± 0.04	2.05 ± 0.02	17.29 ± 0.56	3,729	–	–

Summary of spatio-temporal parameters obtained from permeabilized fibers under isosmotic conditions and in intact fibers subjected to hyperosmotic conditions. See text for further explanation
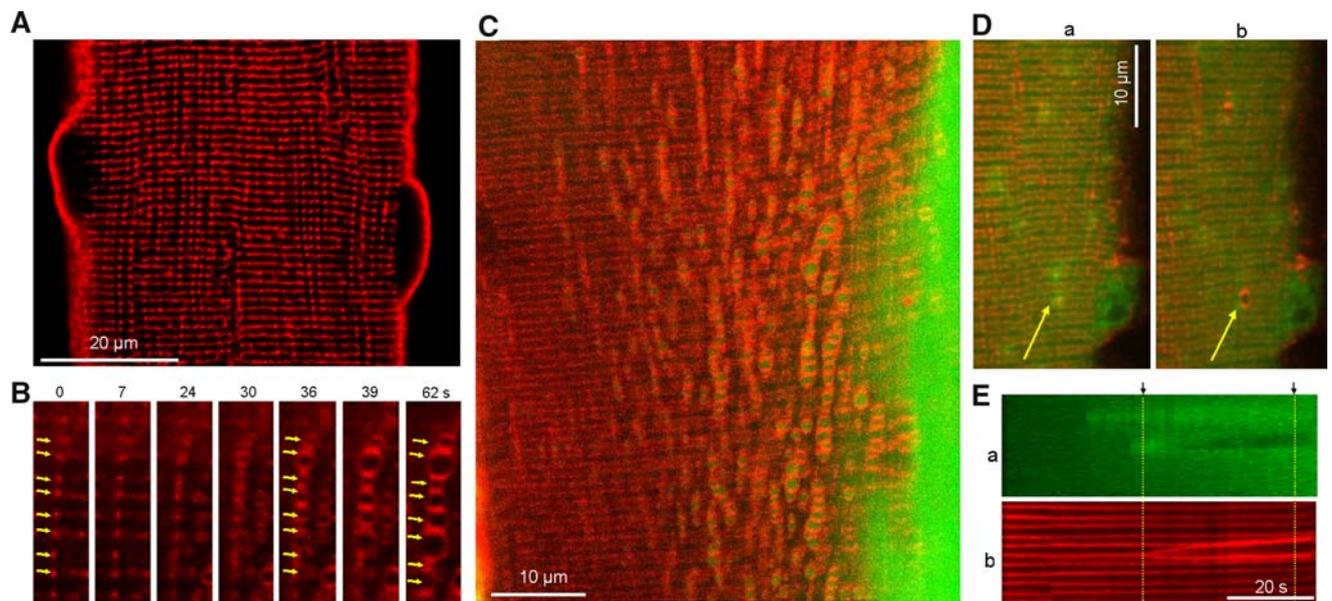

Fig. 5 T-tubular dilation accompanying ECRE under hyperosmotic conditions. **A** Section of an isolated muscle fiber showing plasma membrane and transverse tubules stained with the fluorescent dye FM4-64. **B** Magnified ROI near the surface of a fiber at different times after exposure to hyperosmotic solution (Ca-HyO). *Arrows* indicate T-tubules undergoing dilation. **C** Peripheral region of a muscle fiber stained with FM4-64 (*red*) and exposed to a hyperosmotic Ringer's solution (S-HyO) containing 100 µM mM fluo-4 (*green*). The appearance of areas stained *green* (from fluo-4 fluorescence) within the fiber indicate dilated T-tubules with free access to the extracellular space. **D** Muscle fiber section stained with extracellular FM4-64 and intracellular fluo-4-AM at two times (see **E**) after application of hyperosmotic solution (S-HyO). The *arrows* indicate an ECRE in a and T-tubule dilation at the same location in *b*, respectively. **E** Reconstructed line scan images obtained from crops of xy-images that contained the region labelled with the arrow in (**D**); panels a and b display the fluo-4 and the FM4-64 channel, respectively. Note the Ca elevation at the beginning of the T-tubule swelling. *Black arrows* and the *vertical lines* indicate the times when images Da and Db were taken

stimulated by hyperosmotic solution. Only a small increase in basal fluorescence could be observed during the challenge (Fig. 6, lower right panel), probably caused by concentrating the dye due to fiber shrinkage. Importantly, none of the fibers tested responded with ECRE (upper right panel). In contrast, fibers in the same series of experiments bathed in Ringer's solution responded with a more than 100% increase in global fluorescence and showed a high percentage of ECRE responsiveness. Thus, conditions that chronically inactivate the DHPR appear to also make the Ca release system refractory to osmotic stress. Reversibility after the long lasting depolarization was tested in five fibers. Three fibers responded again with ECRE on return to Ringer's solution.

Hypertonicity-induced TT swelling and Ca signals in myotubes

A second approach to gain information about the role of the DHPR is studying muscle cells deficient of this protein. As
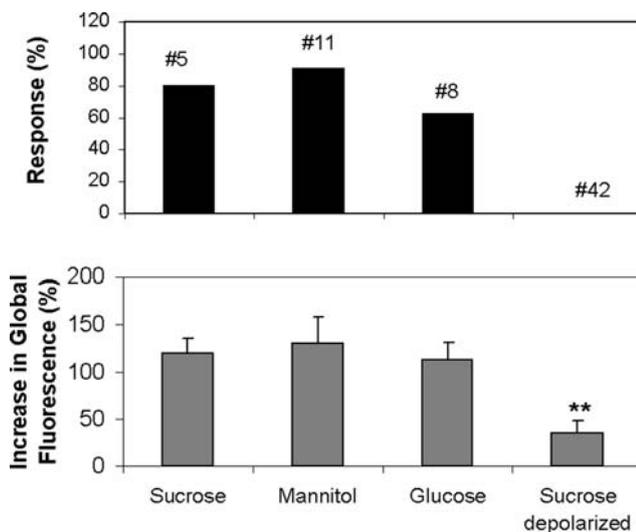
Fig. 6 Local Ca response suppressed by depolarization Response of local (*upper panel*) and global (*lower panel*) fluo-4 signals to hyperosmotic stress (420 mOsm) in isolated muscle fibers under conditions that favor a normal resting potential (*left and middle columns*) and under depolarizing conditions (*right columns*). At normal polarization, the responsiveness was high (regardless whether osmolarity was raised by sucrose, mannitol or glucose). However, depolarization strongly suppressed the response. ** indicates significant difference ($P < 0.01$)

DHPR-deficiency is not compatible with postnatal survival (Adams and Beam, 1990), we studied cultured skeletal myotubes with and without DHPR. Figure 7 depicts experimental results from a myotube cultured from the mouse-derived myogenic cell line C2C12 (Blau et al. 1983). Myotubes of this line show a well-developed DHPR-mediated Ca release (Schuhmeier et al. 2003). The procedure was similar to the one described for fibers: The membrane portions with access to the extracellular solution were first labeled with externally applied FM4-64; then an external solution containing 0.1 mM fluo-4 was applied and the extracellular osmolarity was rapidly increased by superfusion from a micropipette. Figure 7A and B show xy-scans of a region of the myotube before and 150 s after raising the osmolarity to 420 mOsm. As in the isolated muscle fibers, plasma membrane and T-tubules are stained red by FM4-64 and the appearance of green domains in B indicates the dilation of T-tubules with free access to the extracellular space. The time course of the tonicity-induced dilation of two selected tubules of the same cell is demonstrated in the crop image shown in C which was constructed from lines (indicated in A) taken from the individual frames of the sequence of xy-scans. This mock line scan image also demonstrates, that the swelling is reversible after returning from the high osmolarity back to normal (290 mOsm).

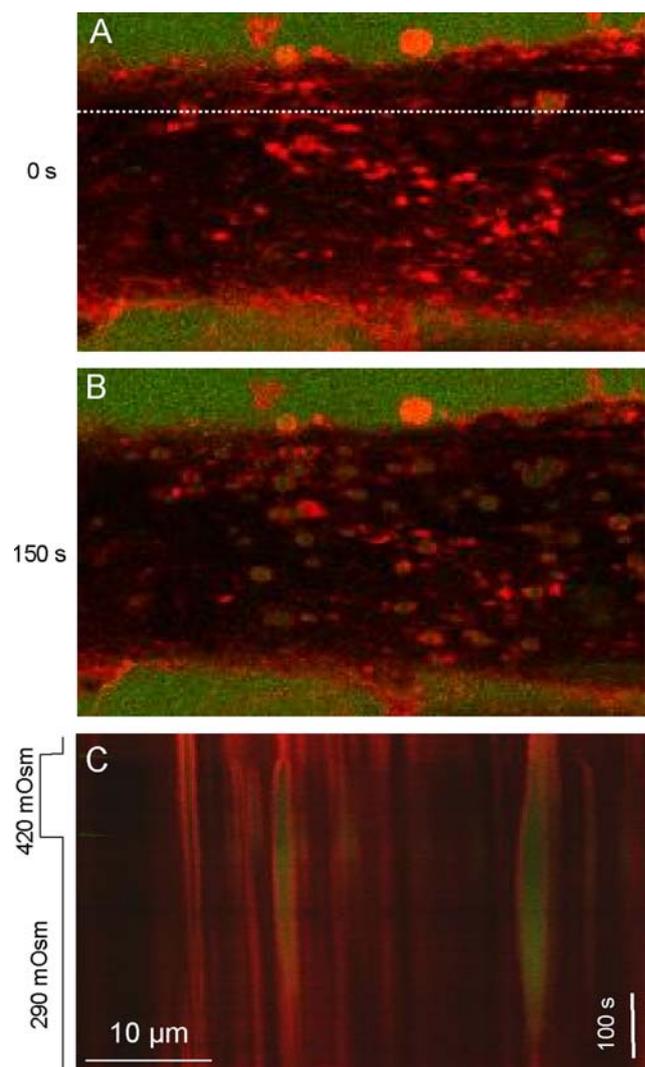Figure 8 shows that C2C12 myotubes responded with local spike-like Ca events and with a concomitant more

Fig. 7 TT swelling in a myotube exposed to hyperosmotic stimulation. **A**, **B** Two confocal xy-images of a time series showing fluorescence from a C2C12 myotube labeled with FM4-64 (*red*) to stain membranes in contact with the extracellular solution. The solution in the extracellular space contained the cell-impermeant variant of Fluo-4 (*green*). The myotube was stimulated by raising the osmolarity to 420 mOsm (S-HyO). **A** Before stimulation. **B** 150 s after application of hyperosmotic solution. Note the *green* circular areas that appear as the result of T-tubular dilation and entry of Fluo-4. **C** xt-image (crops) constructed from *single lines* (indicated in **A**) showing the time course of TT dilation

widespread global fluorescence change as observed in muscle fibers. Figure 8A, B and C are frames obtained before (A) and after (B) commencement of the hyperosmotic stimulus. Panel D is a xt-plot constructed from crops of the xy-scans as described before, demonstrating a pattern of localized Ca elevations that merge into a more continuous fluorescence increase. Figure 8E and F present a quantification of the signals (as shown in Fig. 2) using pooled data from cells responding to the stimulus with ECRE. Global fluorescence intensity (panel a) was determined from a selected

Fig. 8 Global and local Ca activity during hyperosmotic stimulation ▶ in C2C12 myotubes. **A–C** Confocal xy-images of a time series showing fluo-4 fluorescence from a C2C12 myotube stimulated with hyperosmotic solution (Ca-HyO). Before (**A**) and 33 (**B**) and 38 s (**C**) after onset of solution application. **D** xt-image constructed from crops (ROI indicated in **A**). **E**, **F** Pooled results of myotube responses to local superfusion using Ca-HyO and S-HyO, respectively. Averaged recordings of fractional increase in global fluorescence (*a*, normalized to the initial values before the solution change) and ECRE activity (*b*). Thin lines and error bars indicate SEM. *c* Cell responsiveness expressed as percentage of cells showing either no detectable response (*N*), local ECRE signals (*L*) global increase in fluorescence (*G*) or oscillations (*O*). Acquisition conditions: 750 lines/s, 1.46 frames/s
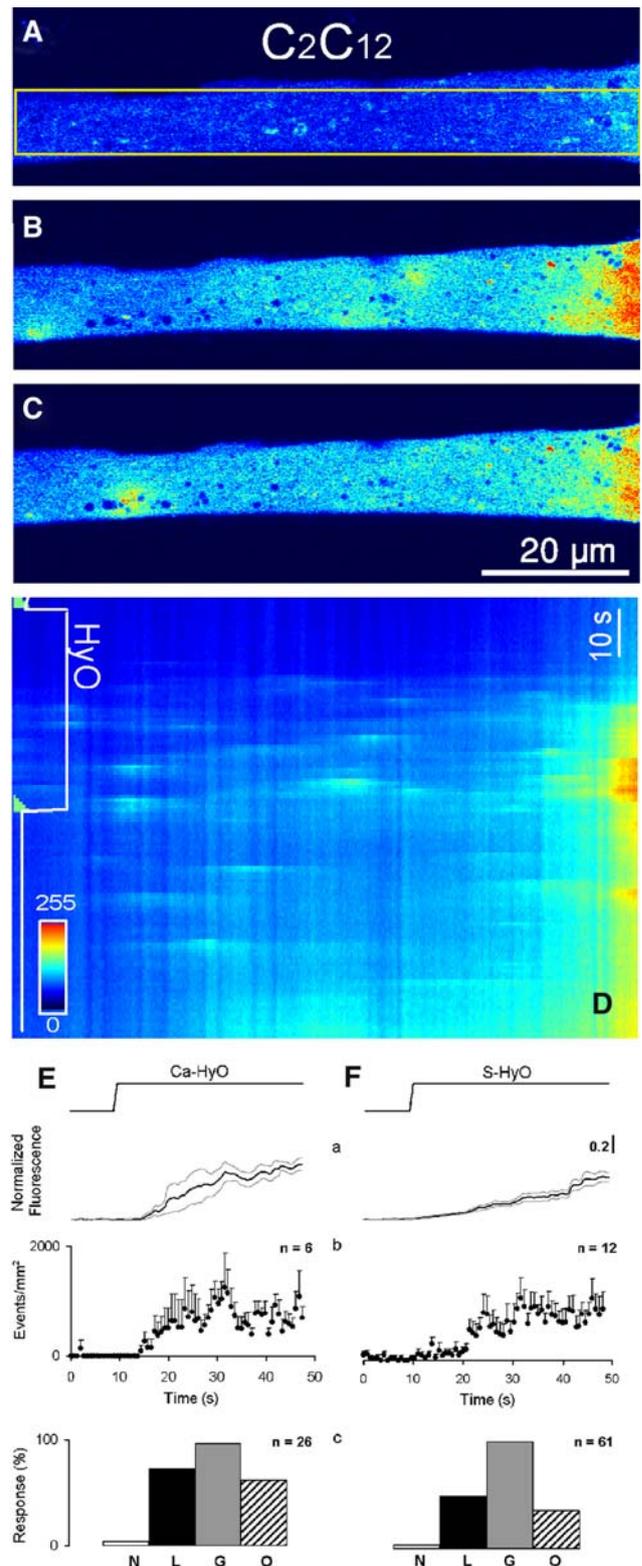
representative ROI of nuclei-free cytoplasm. The pixel intensities within the ROI were averaged and normalized to the intensity average of the initial 15 frames in the series. Local events per frame were counted and normalized by the area of the optical section of the cell (panel b). There were only gradual differences regarding the type of stimulus used, i.e. whether Ca-HyO or S-HyO was applied. A characteristic of the Ca signaling in C2C12 myotubes that differed from the mature fibers was the occurrence of periodic oscillations of large amplitudes. The percentage of cells exhibiting these oscillations was similar to the fraction of cells that showed local ECRE events (Fig. 8E and F, panel c).

Comparison of tonicity-induced local Ca signals in myotubes and muscle fibers

Although the Ca responses elicited by hyperosmotic solution in myotubes resembled those observed in fibers, their spatio-temporal characteristics showed differences. Figure 9A and B show line scan recordings at high time resolution (750 lines/s) from C2C12 myotubes and from a muscle fiber, respectively. The scans were recorded when the changes in diameter, induced by the hyperosmotic solution had settled. In both preparations, short events, lasting less then 100 ms and longer events, lasting several 100 ms, could be noticed. Figure 9C and D compare events in myotubes and fibers at a 100-fold slower time scale. These are "line"-scans constructed from crops of xy-images as described earlier. Comparing A with B and C with D it is evident that both the spatial extent of the local events and their duration are higher in myotubes (C) compared to fibers (D). It should be noted that in Fig. 9C and D, the time resolution is not sufficient to resolve the very short events imaged in panels A and B.

Tonicity-induced Ca signals in DHP-receptor deficient myotubes

Next, we studied DHPR-deficient myotubes. We used myotubes of the cell line GLT (Powell et al. 1996) which

was derived from myoblasts of mice exhibiting the muscular dysgenesis mutation (mdg). These mice harbor a natural deletion mutation that eliminates expression of the
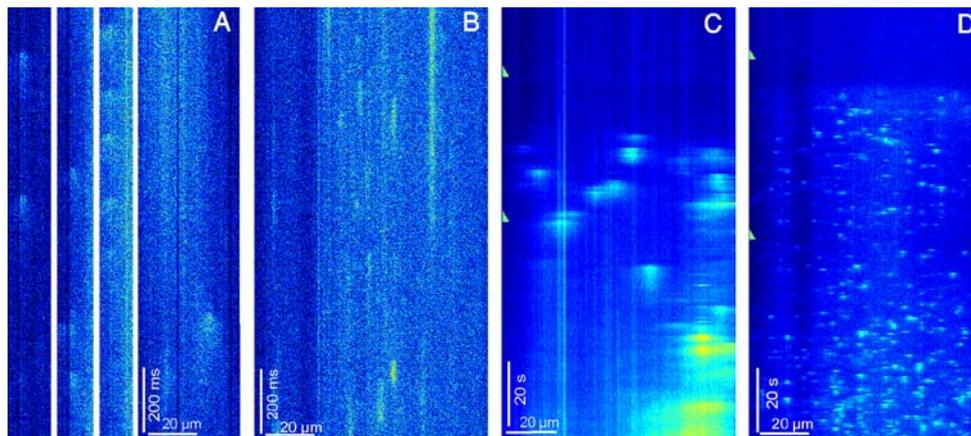
Fig. 9 Comparison of tonicity-induced local Ca signals in myotubes and muscle fibers. **A** xt-images (750 lines/s) of fluo-4-loaded C2C12 myotubes during stimulation with hypertonic solution (Ca-HyO). **B** xt-image of a fluo-4-loaded muscle fiber recorded under identical conditions. **C**, **D** Space-time images of a myotube and a fiber, respectively, constructed from sequences of xy-images (750 lines/s) using frame crops (each line is the average of 15 adjacent lines in the original xy image)

alpha1S subunit of the L-type Ca channel (Beam et al. 1986; Knudson et al. 1989; Chaudhari 1992).

The xy-scans of Fig. 10 were obtained from a GLT myotube before (A) and 12 (B), 16 (C) and 68 s (D) after the onset of the solution ejection. ECRE responses can be observed at different locations of the cell combined with a gradual global rise in fluorescence. Figure 10E and F quantify the responses as shown in Fig. 8E and F. When the high-Ca solution used by Wang et al. (2005) was applied, local events emerged in about half of the cells tested. However the ECRE activity found in these cells was lower than in C2C12 cells under identical conditions. A strongly distinct response pattern was obtained when sucrose was used to raise the osmolarity. Whereas every other C2C12 myotube showed ECRE under these conditions, only a minor fraction of the GLT myotubes responded. Together with the ECRE responsiveness, the number of cells showing oscillations was strongly reduced. Thus, like DHP receptor inactivation in myofibers, the lack of DHP receptors in myotubes appears to exert a suppressing effect on local Ca transients during osmotic stress.

Discussion

Tonicity-induced Ca signals in mouse muscle fibers

In the first part of this study, we focused on the conditions to elicit microdomain calcium signals by hyperosmotic stress in mouse muscle fibers (Wang et al. 2005) and on their spatio-temporal characteristics. The extent of fiber shrinkage and the parameters of the local calcium signals that appeared in the cell periphery were not substantially different when comparing the trigger conditions of Wang et al. (2005) (Ca-HyO) with those avoiding ionic strength changes by using sugars (predominantly sucrose, S-HyO) in an otherwise identical experimental setting. Yet, the ECRE responsiveness (Fig. 2) and the event density (Table 1) were higher in Ca-HyO compared to S-HyO indicating a contribution of the high extracellular calcium concentration to the efficiency of the osmotic stress. A surprising feature of muscle fibers stimulated with S-HyO vs. Ca-HyO was an increase in the global Ca concentration (corresponding to a uniform increase in fluorescence by $110 \pm 40\%$) that occurred in addition to the local ECRE. Depolarization of the fiber membrane, a possible reason for a widespread elevation in basal Ca, seems unlikely as an explanation because careful measurements by Teichmann et al. (2008) showed a slight hyperpolarization rather than a depolarization under similar conditions.

Comparing ECRE elicited by hyper-osmotic stress in intact fibers with those appearing spontaneously in permeabilized fibers using the procedure of Kirsch et al. (2001), a large part of the events were found to be short and spark-like in both cases. However, a hallmark of the Ca activity induced by osmotic stress both with Ca-HyO and S-HyO was the additional frequent presence of signals with similar amplitudes but much longer durations reaching several hundreds of milliseconds (see Fig. 4B and C). Similar characteristics were reported for the local Ca signals observed after the return to iso-osmotic conditions after a short strong hypo-osmotic challenge (Weisleder et al. 2007).

Alterations in transverse tubular morphology by hypertonic solutions

Our finding of TT dilations in mouse fibers are in accord with ultra-structural investigations in frog muscle fibers
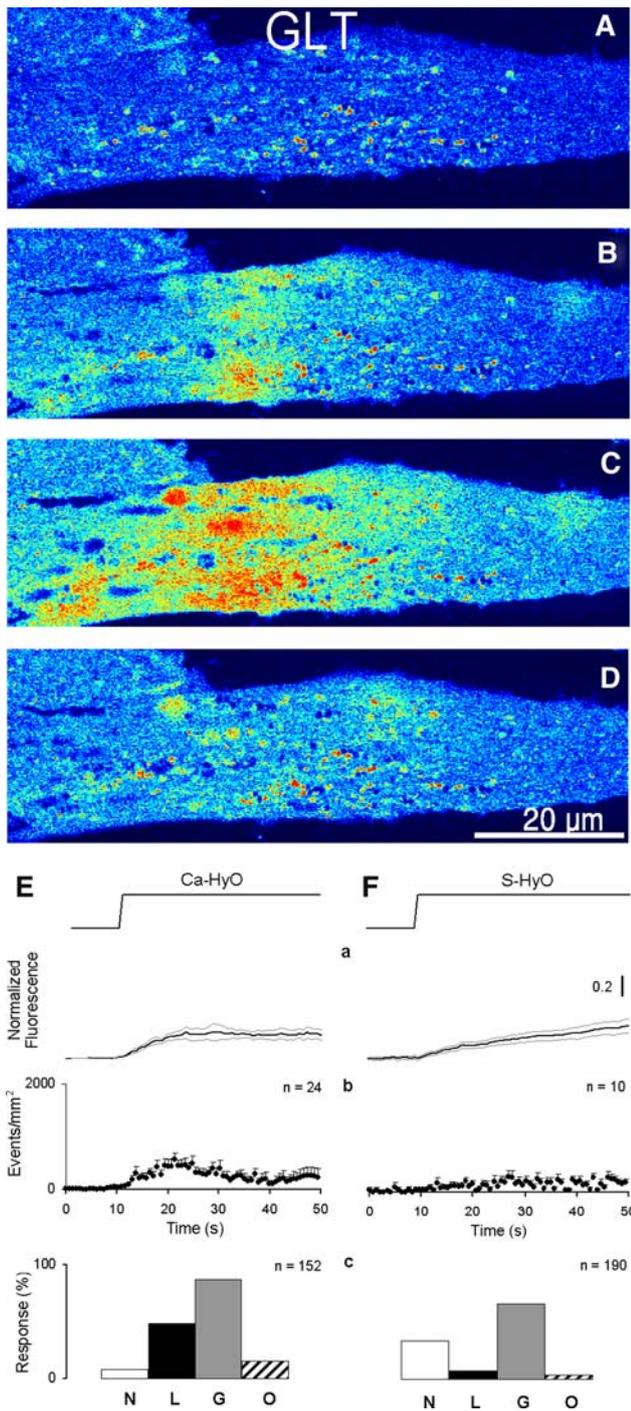
Fig. 10 Ca signals in response to hyperosmotic stimulation in myotubes deficient in the DHP receptor alpha1-subunit. **A–D** Confocal xy-scans of a DHPR-deficient GLT myotube before and 12, 16, and 68 s after the onset of superfusion with Ca-HyO, respectively. **E, F** Pooled data of myotube response using Ca-HyO and sucrose S-HyO, respectively. See description of Fig. 8. Thin lines and error bars indicate SEM

exposed to hyper-osmotic solutions (Martin et al. 2003). Under highly hyper-tonic conditions (addition of 350 mM sucrose for 30 min) electron micrographs showed marked

dilation and vacuolation of the T-tubules combined with SR shrinkage, whereas milder conditions (100 mM sucrose) similar to ours caused less dilated T-tubules and smaller reductions in SR volume. Our local perfusion experiments traced the dynamic onset of the structural alterations in the TT. Apparently, the hyper-osmotic solution, when entering the tubules, causes a rapid water outflow, predominantly from the near-surface intracellular space, leading to tubule dilation in the peripheral fiber regions. Our finding of ECRE co-localized with TT dilation (Fig. 5D and E) is further evidence that the deformations of the T-tubular membrane and the Ca signals are causally related. Even though the expansion of the TT showed a rapid onset, it lagged behind the ECRE activity. Nevertheless, we think that volume changes are the initial mechanical event for the generation of the local Ca signals. Probably the initial phase of dilation, below the resolution of the optical microscope, is sufficient to induce transient ECRE activity. Figure 2 (row c) shows that the mean ECRE activity reaches its maximal value before the corresponding volume change approaches its final value. This likewise indicates that relatively small volume changes are sufficient to induce local Ca transients. In fact, we found that also considerably lower osmolarities were sufficient to induce ECRE, yet at a much reduced success rate.

Osmotic stress situations occur during physiological conditions in skeletal muscle. Strenuous activity leads to the extrusion of osmotically active substances. Vacuole formation, caused by local deletions of the TT system has been observed in Xenopus skeletal muscle following fatiguing activity (reviewed by Lannergren et al. 2002) and has been attributed to the accumulation of osmolytes, in particular lactate, in the TT lumen (Lannergren et al. 2000). Mammalian unlike amphibian muscle showed no vacuole formation under identical conditions. TT dilations were, however, noticable when external lactate was applied during the fatiguing activity indicating that normally lactate may be too rapidly extruded from the TT lumen for vacuolation to occur (Lannergren et al. 2000). Still, volume changes too subtle to be detected in the confocal images may cause alterations of the triadic micro-structure. Such changes have been suggested by Lannergren et al. (2002) to influence excitation-contraction coupling explaining the loss of force in low frequency fatigue. Experiments assessing ultra-structural changes of frog muscle triads after fatiguing activity, that revealed increases in TT diameter below the resolution of the light microscope and an increase in TT-SR distance, support this view (Usher-Smith et al. 2007).

Role of the DHP receptor in tonicity-induced Ca signals

The large changes in transverse tubular morphology observed here might explain the local Ca fluctuations by

unspecific membrane damage. Several lines of previous evidence, however, point to the involvement of specific signaling mechanisms in their generation. A participation of cytoskeletal elements is indicated by the studies of Wang et al. (2005) and Teichmann et al. (2008) showing much stronger responses in dystrophin-deficient mdx muscle fibers. ECRE persisted in Ca-free external solution, making the SR the likely source of Ca for these fluctuations (Teichmann et al. 2008; Weisleder and Ma 2006). Experiments by Martins et al. (2008) point to the participation of reactive oxygen species (ROS) resulting from NADPH-oxidase (NOX) activity in the generation of tonicity-induced ECRE. NOX is expressed in the T-tubular region of skeletal muscle (Hidalgo et al. 2006). Finally, using a specific blocker, Teichmann et al. (2008) provided evidence for a role of mechano-sensitive channels as part of the transduction process that leads to ECRE in mdx fibers. They suggested a model incorporating all these elements and proposed the DHPR-RyR1 connection as the final target for the mechanical response. The DHPR (L-type Ca channel) normally serves as the voltage sensor for the depolarization-activated Ca release and is thought to be mechanically coupled to the RyR1. Consistent with the hypothesis that the physical contact between DHPR and RyR forms also the basis for the tonicity-induced local Ca signals (Wang et al. 2005, Teichmann et al. 2008), we found that chronic depolarization, which converts the DHPR to an inactivated conformational state, reversibly prevented the Ca response to osmotic stress. According to the experiments in frog muscle performed by Martin et al. (2003) the ultra-structure of the T-SR junction remains unchanged during even much higher hypertonicity (350 mM sucrose) despite obvious alterations in TT and SR volume. Therefore, it seems feasible that the DHPR-RyR1 contact is not lost during osmotic stress and that the tonicity-induced SR Ca release remains under partial control of the DHPR and can be suppressed by DHPR inactivation.

A further piece of evidence in favor of DHPR involvement in the osmotic stress response is our finding that DHPR-deficient cells show lower ECRE activity than normal myotubes when challenged by hyper-osmotic solutions. GLT myotubes, unlike normal myotubes, were almost completely unresponsive to hyperosmotic stimulation using S-HyO. On the other hand, they showed ECRE when stimulated with Ca-HyO, indicating that the DHPR alpha1 subunit is, even though apparently important, not essential for the mechanism evoking these signals. Other structural links between TT and SR obviously exist because triad formation between these two membrane compartments is maintained in the absence of the DHPR in GLT-myotubes (Powell et al. 1996). These structures may convey a mechanical gating of Ca release caused by the volume increase of the TT system that we see under hyperosmotic conditions.

Conclusions

In summary, we investigated properties and prerequisites of local Ca signals (ECRE) in mammalian muscle cells induced by hypertonic stress. Sites of ECRE were associated with a substantial dilation of nearby transverse tubules and ECRE activity was eliminated by long-lasting depolarization that inactivates the DHPR and were strongly reduced in DHPR-deficient myotubes. Yet, the incomplete inhibition of ECRE in these myotubes (in particular under high-Ca conditions) suggests that the specific interaction between DHPR and ryanodine receptors is not absolutely necessary for the tonicity-induced Ca response to occur. The effect may be mediated by other protein links between the T-system and the SR but modulated by the DHPR voltage-dependent states.

References

Adams BA, Beam KG (1990) Muscular dysgenesis in mice: a model system for studying excitation-contraction coupling. FASEB J 4:2809–2816

Beam KG, Knudson CM, Powell JA (1986) A lethal mutation in mice eliminates the slow calcium current in skeletal muscle cells. Nature 320:168–170. doi:10.1038/320168a0

Blau HM, Chiu CP, Webster C (1983) Cytoplasmic activation of human nuclear genes in stable heterocaryons. Cell 32:1171–1180. doi:10.1016/0092-8674(83)90300-8

Chaudhari N (1992) A single nucleotide deletion in the skeletal muscle-specific calcium channel transcript of muscular dysgenesis (mdg) mice. J Biol Chem 267:25636–25639

Chawla S, Skepper JN, Hockaday AR, Huang CL (2001) Calcium waves induced by hypertonic solutions in intact frog skeletal muscle fibres. J Physiol 536:351–359. doi:10.1111/j.1469-7793.2001.0351c.xd

Csernoch L, Zhou J, Stern MD, Brum G, Rios E (2004) The elementary events of Ca^{2+} release elicited by membrane depolarization in mammalian muscle. J Physiol 557:43–58. doi:10.1113/jphysiol.2003.059154

Dulhunty AF (1991) Activation and inactivation of excitation-contraction coupling in rat soleus muscle. J Physiol 439:605–626

Dulhunty AF (2006) Excitation-contraction coupling from the 1950s into the new millennium. Clin Exp Pharmacol Physiol 33:763–772. doi:10.1111/j.1440-1681.2006.04441.x

Hidalgo C, Sanchez G, Barrientos G, Aracena-Parks P (2006) A transverse tubule NADPH oxidase activity stimulates calcium release from isolated triads via ryanodine receptor type 1 S-glutathionylation. J Biol Chem 281:26473–26482. doi:10.1074/jbc.M600451200

Kirsch WG, Uttenweiler D, Fink RH (2001) Spark- and ember-like elementary Ca^{2+} release events in skinned fibres of adult mammalian skeletal muscle. J Physiol 537:379–389. doi:10.1111/j.1469-7793.2001.00379.x

Klein MG, Schneider MF (2006) Ca^{2+} sparks in skeletal muscle. Prog Biophys Mol Biol 92:308–332. doi:10.1016/j.pbiomolbio.2005.05.016

Klein MG, Cheng H, Santana LF, Jiang YH, Lederer WJ, Schneider MF (1996) Two mechanisms of quantized calcium release in skeletal muscle. Nature 379:455–458. doi:10.1038/379455a0

Knudson CM, Chaudhari N, Sharp AH, Powell JA, Beam KG, Campbell KP (1989) Specific absence of the alpha 1 subunit of the dihydropyridine receptor in mice with muscular dysgenesis. J Biol Chem 264:1345–1348

Lannergren J, Bruton JD, Westerblad H (2000) Vacuole formation in fatigued skeletal muscle fibres from frog and mouse: effects of extracellular lactate. J Physiol 526(Pt 3):597–611. doi:10.1111/j.1469-7793.2000.00597.x

Lannergren J, Westerblad H, Bruton JD (2002) Dynamic vacuolation in skeletal muscle fibres after fatigue. Cell Biol Int 26:911–920. doi:10.1006/cbir.2002.0941

Martin CA, Petousi N, Chawla S, Hockaday AR, Burgess AJ, Fraser JA, Huang CL, Skepper JN (2003) The effect of extracellular tonicity on the anatomy of triad complexes in amphibian skeletal muscle. J Muscle Res Cell Motil 24:407–415. doi:10.1023/A:1027356410698

Martins AS, Shkryl VM, Nowycky MC, Shirokova N (2008) Reactive oxygen species contribute to Ca^{2+} signals produced by osmotic stress in mouse skeletal muscle fibres. J Physiol 586:197–210. doi:10.1113/jphysiol.2007.146571

Melzer W, Herrmann-Frank A, Lüttgau HC (1995) The role of Ca^{2+} ions in excitation-contraction coupling of skeletal muscle fibres. Biochim Biophys Acta 1241:59–116

Powell JA, Petherbridge L, Flucher BE (1996) Formation of triads without the dihydropyridine receptor alpha subunits in cell lines from dysgenic skeletal muscle. J Cell Biol 134:375–387. doi:10.1083/jcb.134.2.375

Schuhmeier RP, Melzer W (2004) Voltage-dependent Ca^{2+} fluxes in skeletal myotubes determined using a removal model analysis. J Gen Physiol 123:33–51. doi:10.1085/jgp.200308908

Schuhmeier RP, Dietze B, Ursu D, Lehmann-Horn F, Melzer W (2003) Voltage-activated calcium signals in myotubes loaded with high concentrations of EGTA. Biophys J 84:1065–1078. doi:10.1016/S0006-3495(03)74923-6

Schuhmeier RP, Gouadon E, Ursu D, Kasielke N, Flucher BE, Grabner M, Melzer W (2005) Functional interaction of CaV channel isoforms with ryanodine receptors studied in dysgenic myotubes. Biophys J 88:1765–1777. doi:10.1529/biophysj.104.051318

Shirokova N, Gonzalez A, Kirsch WG, Rios E, Pizarro G, Stern MD, Cheng H (1999a) Calcium sparks: release packets of uncertain origin and fundamental role. J Gen Physiol 113:377–384. doi:10.1085/jgp.113.3.377

Shirokova N, Shirokov R, Rossi D, Gonzalez A, Kirsch WG, Garcia J, Sorrentino V, Rios E (1999b) Spatially segregated control of Ca^{2+} release in developing skeletal muscle of mice. J Physiol 521(Pt 2):483–495. doi:10.1111/j.1469-7793.1999.00483.x

Teichmann MD, Wegner FV, Fink RH, Chamberlain JS, Launikonis BS, Martinac B, Friedrich O (2008) Inhibitory control over Ca(2+) sparks via mechanosensitive channels is disrupted in dystrophin deficient muscle but restored by mini-dystrophin expression. PLoS ONE 3:e3644. doi:10.1371/journal.pone.0003644

Usher-Smith JA, Fraser JA, Huang CL, Skepper JN (2007) Alterations in triad ultrastructure following repetitive stimulation and intracellular changes associated with exercise in amphibian skeletal muscle. J Muscle Res Cell Motil 28:19–28. doi:10.1007/s10974-007-9100-2

Vida TA, Emr SD (1995) A new vital stain for visualizing vacuolar membrane dynamics and endocytosis in yeast. J Cell Biol 128:779–792. doi:10.1083/jcb.128.5.779

Wang X, Weisleder N, Collet C, Zhou J, Chu Y, Hirata Y, Zhao X, Pan Z, Brotto M, Cheng H, Ma J (2005) Uncontrolled calcium sparks act as a dystrophic signal for mammalian skeletal muscle. Nat Cell Biol 7:525–530. doi:10.1038/ncb1254

Weisleder N, Ma JJ (2006) Ca^{2+} sparks as a plastic signal for skeletal muscle health, aging, and dystrophy. Acta Pharmacol Sin 27:791–798. doi:10.1111/j.1745-7254.2006.00384.x

Weisleder N, Ferrante C, Hirata Y, Collet C, Chu Y, Cheng H, Takeshima H, Ma J (2007) Systemic ablation of RyR3 alters Ca^{2+} spark signaling in adult skeletal muscle. Cell Calcium 42:548–555. doi:10.1016/j.ceca.2007.01.009

Zhou J, Brum G, Gonzalez A, Launikonis BS, Stern MD, Ríos E (2003) Ca^{2+} sparks and embers of mammalian muscle. Properties of the sources. J Gen Physiol 122:95–114. doi:10.1085/jgp.200308796

Zhou J, Yi J, Royer L, Launikonis BS, Gonzalez A, Garcia J, Rios E (2006) A probable role of dihydropyridine receptors in repression of Ca^{2+} sparks demonstrated in cultured mammalian muscle. Am J Physiol Cell Physiol 290:C539–C553. doi:10.1152/ajpcell.00592.2004